Solar-Terrestrial Physics. 2025, vol. 11, iss. 3, pp. 114–119. DOI: 10.12737/stp-113202513. © 2025 A.V. Stepanov, V.V. Zaitsev. Published by INFRA-M Academic Publishing House

DOI: 10.12737/stp-113202513

Received March 04, 2025
Accepted April 03, 2025

THE RAYLEIGH — TAYLOR INSTABILITY AS A TRIGGER OF SOLAR FLARES

A.V. Stepanov
Central Astronomical Observatory at Pulkovo, St. Petersburg, Russia, stepanov@gaoran.ru
Ioffe Institute, St. Petersburg, Russia

V.V. Zaitsev
Institute of Applied Physics RAS, Nizhny Novgorod, Russia, za130@ipfran.ru

Abstract. The review of authors' papers is devoted to the essential role of the Rayleigh — Taylor instability (RTI) as a trigger of flare energy release. We have analyzed two cases of RTI: near coronal loop footpoints and at the loop top. RTI near loop footpoints requires pre-heating of chromospheric plasma. This pre-heating can be realized due to Joule dissipation in partially ionized plasma under condition of the Cowling resistivity. RTI at the loop top arises in current-carrying coronal loop loaded by prominence. We have determined the conditions of RTI as a flare trigger in both cases. It is shown that RTI generates super-Dreicer electric field in the chromospheric parts of a loop. This is the promising solution of longstanding "number problem" of particle acceleration. RTI can be also a cause of prompt (~10 s) hot onset precursor events (HOPE).

Keywords: Sun, flare trigger, Joule dissipation, particle acceleration.

INTRODUCTION

The epigraph to this review article is a quotation from Cornelis de Jager "Flares are different". Indeed, the observed variety of flares does not fit into the Procrustean bed of the standard model. In recent decades, it has been found that in most flares flare plasma is heated before the appearance of hard X-ray caused by electrons accelerated in a flare [Veronig et al., 2002; Sharykin, Kosovichev, 2015; Meshalkina, Altyntsev, 2024]. Moreover, in some cases there is unusually rapid (~10 s) pre-flare heating of chromospheric plasma up to 10–15 MK at coronal magnetic loop footpoints [Hudson et al., 2021]. A number of recent works have examined the nature of hot onset precursor events (HOPE) (see, e.g., [da Silva et al., 2023; Battaglia et al., 2023]). Nevertheless, the mechanism of the rapid heating has not been determined yet.

The problem of explaining the huge number of charged particles accelerated in a flare remains unclear in the physics of solar flares [Hoyng et al., 1976]. It has been established that a solar flare in the impulsive phase produces ~10^{37} energetic (>20 keV) electrons per second, and the total number of such electrons during the impulsive phase (~100 s) is 10^{39}[Miller et al., 1997]. This exceeds the number of thermal electrons in the coronal part of the magnetic loop: $(1\div5)10^{37}$ [Emslie, Henoux, 1995]. In giant flares, the number of electrons with energies >20 keV can be as large as 10^{41} [Kane et al., 1995], i.e. the entire plasma in the flare loop should be in acceleration mode. One possible solution to this problem is acceleration in denser layers of the solar atmosphere.

An important problem is to identify the trigger of solar flares. A number of possible flare triggers have been discussed in the literature: thermal trigger [Syrovatskii, 1976; Ledentsov, 2021], topological trigger [Somov, 2008; Kusano et al., 2012], interaction between magnetic loops [Kumar et al., 2010], trigger prominence [Pustil'nik, 1974; Zaitsev, Stepanov, 1992]. In this paper, we investigate the role of Rayleigh — Taylor instability (RTI) as a solar flare trigger in the typical magnetic configuration — the current-carrying flare loop. We examine two cases of RTI development: near loop footpoints and at its top due to prominence activity. We also study two important consequences of RTI development as a flare trigger: plasma heating due to Joule dissipation and acceleration of charged particles.

RAYLEIGH — TAYLOR INSTABILITY AT FLARE LOOP FOOTPOINT

We proceed from the representation of a flare loop as an equivalent electric circuit [Alfvén, Carlqvist, 1967], when an electric current is generated by convective motions in the photosphere, and the current flowing through the loop is closed either through the photosphere at the level of $\tau_{5000}=1$ [Zaitsev, Stepanov, 1992; Zaitsev et al., 2020] or through the loop surface [Melrose, 1991]. Figure 1 schematically shows a flare loop footpoint located in the partially ionized chromosphere. RTI is caused by centrifugal acceleration with an appropriate magnetic field curvature with radius R_c [Zaitsev, Stepanov, 2015]:

$$\vec{g}_c = \frac{\vec{f}_c}{\rho} = \frac{2k_B T}{m_i R_c^2}\frac{n}{n+n_a}\vec{R}_c, \quad (1)$$

where ρ is the plasma number density; k_B is the Boltzmann constant; T is the plasma temperature at the outer boundary of the flux tube; n, n_a are electron and neutral atom densities respectively. The appropriate curvature of the magnetic field of a loop is formed in the region of a sharp increase in the width of the loop due to a decrease in external pressure; therefore, the vertical size of the RTI region can be estimated as $l\approx(0.5\div1.0)\ 10^8$ cm. The dynamic pressure gradient of the convective flow

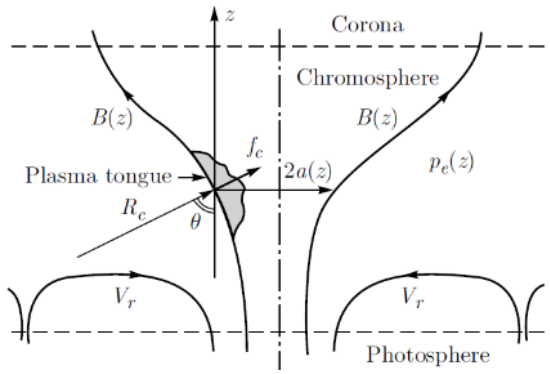

Figure 1. Scheme of plasma injection from the chromosphere into the magnetic loop footpoint during the development of RTI: f_c is the centrifugal force; $a(z)$ is the radius of the magnetic flux tube; p_e is the external gas pressure; θ is the angle between the direction of the radius of curvature and the vertical [Zaitsev, Stepanov, 2015]

also acts on the outer boundary of the tube. $-m_i\left(n+n_a\right)\partial V_r^2/\partial r$. Assuming $V_r(r,t)=-V_0(t)r/a$, we obtain the condition for RTI development (ballooning mode) $g_c+\dfrac{2V_0^2}{a}\sin\theta-g\cos\theta>0$, which at $H\left(z\right)=\dfrac{k_B T_e\left(z\right)}{m_i g}>a\left(z\right)$ takes the form [Zaitsev, Stepanov, 2015]:

$$\frac{nT}{2\left(n+n_a\right)T_e}+\frac{8HV_0^2\left(t\right)}{a^2 g}>1. \tag{2}$$

Here, T_e is the temperature inside the magnetic flux tube; g is acceleration of gravity on the Sun. It follows from (2) that ballooning instability develops when the outer shell of the flux tube is heated and the convective plasma flow velocity (dynamic force) increases sharply. To determine the temperature to which the outer shell should be heated, we can use the modified Saha formula for hydrogen atom [Brown, 1973]:

$$\frac{\left(n+n_a\right)x^2}{1-x}= 7.2\cdot10^{18}T^{1/2}\exp\left(-6.583-\frac{1.185\cdot10^5}{T}\right), \tag{3}$$

where $x=n/(n+n_a)$ is the degree of ionization. It follows from (3) that for a chromospheric layer with a density $n+n_a=10^{15}$ cm^{-3} instability criterion (2) is fulfilled at relatively low plasma stream velocities $V_0(t)$ if the flux tube shell is heated to $T\approx2.5\cdot10^4$ K. The degree of ionization x runs to 90 %, and the instability criterion takes the form $xT/(2T_e)\approx2.6>1$. In this case, the typical RTI time in the magnetic flux tube with radius $a\approx\left(3\div5\right)10^7$ cm

$$\tau_{RT}\approx\left(3^{3/2}aT_e/4\pi Tg\right)^{1/2}\approx10\text{ s}. \tag{4}$$

This value is of the order of a/V_{Ti} that takes the external plasma tongue to penetrate the magnetic flux tube with the thermal velocity of ions.

The Rayleigh — Taylor instability causes disturbance of the magnetic field of a loop and compression of the current channel leading to amplification of current and its increased dissipation due to ion-neutral particle collisions in chromospheric plasma.

ELECTRON ACCELERATION IN INDUCED ELECTRIC FIELDS

Electric field acceleration of charged particles is most effective. When the chromospheric plasma tongue penetrates into the loop footpoint at a velocity $V_r\left(r,t\right)=-V_0\left(t\right)r/a$ the magnetic field components B_z and $B_\varphi=2I/(ca)$, and hence the current, according to $\partial\vec{B}/\partial t=\text{rot}\left[\vec{V}\times\vec{B}\right]$, evolve as follows:

$$\begin{aligned} B_\varphi\left(r,t\right)&=B_{\varphi0}\frac{r}{a}\exp\left(\frac{2}{a}\int_0^t V_0\left(t'\right)dt'\right),\\ B_z\left(r,t\right)&=const\cdot\exp\left(\frac{2}{a}\int_0^t V_0\left(t'\right)dt'\right). \end{aligned} \tag{5}$$

From Formula (5) and $\text{rot}\,\vec{E}=-\left(1/c\right)\partial\vec{B}/\partial t$, we can show that with the development of RTI the induced electric field $\vec{E}=-\left(1/c\right)\left[\vec{V}\times\vec{B}\right]$ is perpendicular to the magnetic field, so it does not accelerate charged particles. However, during the time $\tau_A\approx l/V_A\approx5\div10$ s, where $l\approx\left(0.5\div1.0\right)10^8$ cm is the vertical extent of the RTI region, the magnetic field tension pulse B_φ "escapes" from the instability region at an Alfvén velocity V_A as a pulse of longitudinal electric current

$$\frac{\partial^2B_\varphi}{\partial t^2}=\frac{B_{z0}^2}{4\pi\rho}\frac{\partial^2B_\varphi}{\partial z^2}. \tag{6}$$

The magnetic pressure pulse $B_z(r,t)$ remains in the region of plasma tongue penetration, exciting FMS oscillations (Figure 2).

If the current is low ($B_\varphi^2\le8\pi p$, where p is the plasma gas pressure), the magnetic field disturbance is balanced by the gas pressure disturbance and $E_z=0$. An electric current pulse propagates along the loop as a linear Alfvén wave. At $B_\varphi^2\gg8\pi p$, an induced electric field appears which is directed along the magnetic field of the loop B_{z0}. This is due to the fact that at $B_\varphi^2\gg8\pi p$ magnetic field disturbances are no longer balanced by the gas pressure gradient as in the linear Alfvén pulse, but velocity perturbations occur along the flux tube radius and along the undisturbed magnetic field B_{z0}, which lead to the generation of the electric field component B_φ nonlinear in field and current along the flux tube axis [Zaitsev et al., 2016]:

$$\frac{\partial E_z}{\partial r}=-\frac{1}{c}\frac{B_\varphi^2}{4\pi\rho V_A^2}\frac{\partial B_\varphi}{\partial t}. \tag{7}$$

The electric field average with respect to the loop cross-section

$$\overline{E_z} = \frac{2I_0^2 V_A}{5c^4 B_{z0}^2}\frac{\partial I_0}{\partial \xi},\ \xi = z - V_A t. \quad (8)$$

For example, for $n_a = 10^{14}$ cm^{-3}, $B_{z0} = 300$ G, $I_0 = 10^{10}$ A, find $\overline{E_z} \approx 0.1$ V/cm, i.e. electrons can accelerate at a length $l \approx (0.5 \div 1.0)10^8$ cm to an energy of ~10 MeV. The ratio of the maximum field to the Dreiser field $E_D = 6 \cdot 10^{-8} n/T$ V/cm, when plasma electrons go into escape mode, is [Zaitsev et al., 2016]

$$\frac{E_{zm}}{E_D} = 2.2 \cdot 10^8 \frac{TI_0^3(A)}{a^2 B_{z0} n^{3/2} \Delta\xi}. \quad (9)$$

Figure 3 displays generation regions of electric fields, large and small Dreiser fields for typical conditions in the chromosphere.

Why are electric fields of the order of the Dreiser field necessary for effective acceleration of particles in a flare? In the chromospheric part of the loop, the number of particles in the column from the temperature minimum to the transition region between the chromosphere and the corona averages ~$5 \cdot 10^{39}$. This is enough to provide injection of the required number of electrons ~10^{39} into the acceleration mode [Miller et al., 1997]. Since the total number of accelerated electrons does not differ much from the total number of particles in the chromospheric part of the loop, this indicates a high efficiency of the acceleration mechanism when the number density of accelerated electrons is comparable in order of magnitude to the background plasma number density. This means that when accelerated by regular electric fields, the fields should either be close to or exceed the Dreiser field. That is why, in sufficiently powerful flares, acceleration of electrons should most likely occur in the chromosphere. Otherwise, it is difficult to explain the high number density of accelerated electrons $n \sim 10^{10}$–10^{11} cm^{-3} with an energy >20 keV. Electric fields larger than the Dreiser field can appear at the front of an electric current pulse generated in a loop due to the development of RTI if the current amplitude exceeds 10^{10}A (see Figure 3). The presented results on particle acceleration in the chromosphere can be considered as *déjà vu* — return to the concept of a chromospheric flare [Giovanelli, 1946; Fritzova-Švestková, Švestka 1967].

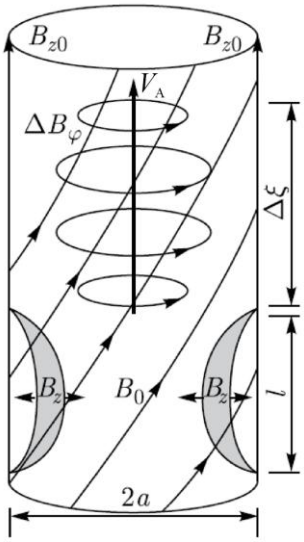

Figure 2. Magnetic field disturbance in the flux tube due to the development of RTI. Here, l is the vertical size of the penetrating external plasma tongue; a is the radius of the magnetic flux tube; $\Delta\xi$ is the size of the electric current pulse along B_{z0} [Zaitsev et al., 2016]

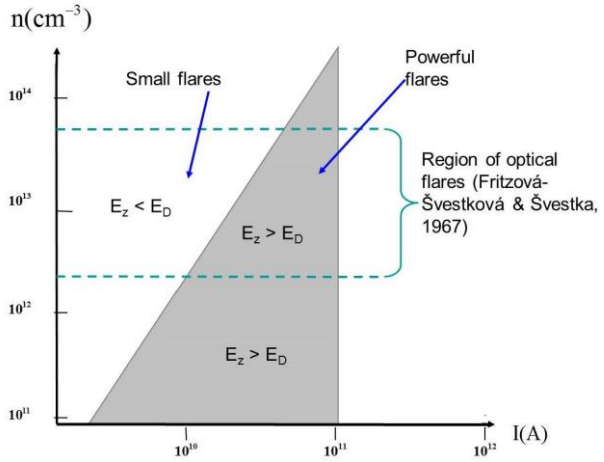

Figure 3. Plasma number density — electric current plot for $a = 10^7$ cm, $B_{z0} = 2 \cdot 10^3$ G, $T = 2 \cdot 10^4$ K, $\delta\Delta\xi = 5 \cdot 10^7$ cm. Regions of sub- and super-Dreicer electric fields (gray) are shown which are formed at the leading edge of a current pulse propagating along a magnetic loop from the RTI region [Zaitsev et al., 2016]

FLARE ENERGY RELEASE INITIATED BY PROMINENCE

Some authors (see, e.g., [Zimovets et al., 2020]) believe that a shortcoming of the current interruption model is the inability to explain the observed energy release at the loop top, which occurs in hard X-ray "above-the-loop-top flare" [Masuda et al., 1994]. We show that RTI caused by prominence at flare loop tops can explain this phenomenon. For the first time, the possibility of initiating a flare in magnetic loops loaded with prominence (filament) was observed by Pustil'nik [1974] under the assumption of magnetic reconnection. In fact, a dense ($n_a + n \sim 10^{11}$–10^{12} cm^{-3}) and relatively cold ($T \sim 0.01$ MK) prominence of thickness $D \approx (3 \div 10)10^8$ cm, located above a flare loop or an arcade of loops with $T \sim (1 \div 10)$ MK and $n \sim 10^9$ cm^{-3}, represents a classical RTI pattern: heavy liquid over light (Figure 4). An appropriate magnetic field curvature is also available. As a result, partially ionized plasma tongues penetrate into the hot current-carrying loop, which lead to increased Joule dissipation under the Cowling resistivity and to acceleration of charged particles, described in the previous section, in induced electric fields. If loops are sequentially arranged in height (see Figure 4), there may occur a Masuda flare effect since the increased plasma number density provides a target thick enough for generating hard X-ray by electrons accelerated at loop tops. This is, briefly, our scenario of a flare trigger due to prominence-induced RTI.

Accordingly, we make some estimates. RTI (ballooning mode) occurs if the prominence thickness $D > D_c = B^2/(10\pi\rho g)$ [Pustil'nik, 1974]. Given $\rho = m_i(n_a + n) = 5 \cdot 10^{-13}$ g/cm^3 and $B = 10$ G, we find $D_c = 2 \cdot 10^8$ cm, which is less than the observed filament thickness.

The Joule dissipation rate per unit volume of magnetic flux tube is determined as [Stepanov, Zaitsev, 2018]

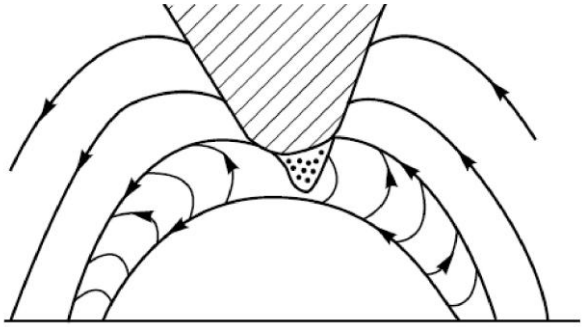

Figure 4. Flare loop-prominence interaction. The tongue of dense partially ionized plasma of prominence penetrates a loop due to RTI [Zaitsev, Stepanov, 1992]

$$q = \left(\mathbf{E} + \frac{1}{c}\mathbf{V}\times\mathbf{B}\right)\mathbf{j} = \\ = \frac{j_z^2}{\sigma} + \frac{F^2 B_\varphi^2 j_z^2}{(2-F)c^2 n m_i \nu'_{ia}}\ \text{erg/(cm}^3\text{s)}, \tag{10}$$

where $j_z = I/(\pi a^2)$, $\sigma = ne^2/(m_e \nu_{ei})$ is the classical conductivity (Spitzer), $F = n_a/(n+n_a)$, $B_\varphi = 2I/(ca)$, $\nu'_{ia} \approx 1.6\cdot 10^{-11} F(n+n_a)\sqrt{T}$. The second term in (10) describes dissipation due to the Cowling resistivity associated with ion-atom collisions, which in the case of injection of neutral particles from a prominence to a magnetic loop is predominant. Then, the dissipation rate can be represented as

$$q = \frac{4F^2 I^4}{(2-F)\pi^2 c^4 a^6 n m_i \nu'_{ia}}\ \text{erg/cm}^3\text{s} \tag{11}$$

Assuming $I=10^{11}$A, $F=0.5$, the loop radius in the corona $a=10^8$ cm, $n=10^9$ cm^{-3}, $T=10^4$ K, we obtain $q\approx 4\cdot 10^3$ erg/(cm ^{3}s). If the energy release region at the loop top is $\sim 3\cdot 10^{25}$ cm^3, we get an energy release capacity of $\sim 10^{29}$ erg/s.

The number of energetic electrons accelerated at the top of the current–carrying loop when the prominence plasma tongue penetrates it can be estimated as $N \approx 2\pi n \Delta x D V_{Ti} \Delta t$. For the time $\Delta t \approx 100$ s at $n \approx 3\cdot 10^{11}$ cm^{-3}, the length of the tongue penetrating the loop top $\Delta x \approx D \approx 3\cdot 10^8$ cm, $V_{Ti}(T = 10^4\ \text{K}) \approx 10^6$ cm/s, we have $N \approx 2\cdot 10^{37}$. This number of accelerated electrons corresponds to a medium power flare.

PULSE HEATING OF THE CHROMOSPHERE AND PROMPT FLARE PRECURSORS

Among HOPEs, there are also unusually prompt flare precursors. For example, Hudson et al. [2021] using observational data from GOES and RHESSI have shown that before the flare impulsive phase on January 7, 2017 the chromospheric coronal magnetic loop footpoints rapidly, for ~10 s, heated up to a temperature 10–15 MK, being almost the same for 1.5 min. The emission measure of radiating loop footpoints slowly increased and, according to GOES data, ran to $n^2V \approx 10^{47}$ cm^{-3}. With loop footpoint volumes of $V \approx 5\cdot 10^{23} \div 10^{25}$ cm^3, this leads to an estimate of plasma number density $n \approx (3.0 \div 4.5)10^{11}$ cm^3 near the precursor region, which is typical of the chromosphere. During the heating phase, the chromosphere was not heated by accelerated electrons. A similar result has been obtained in a number of other papers [Awasthi, Jain, 2011; Battaglia et al., 2023]. Thus, pre-flare heating is not related to collisional heating of the active region by non-thermal electrons, which contradicts the standard flare model.

We assume that the pre-flare heating is linked to a sharp increase in the longitudinal electric current (B_φ) during the development of RTI, described in the previous sections, at loop footpoints. A pulse of high-amplitude longitudinal electric current remains in the chromosphere for $\tau_A \approx l/V_A \approx 5 \div 10$ s. During this time, the current heats the chromospheric footpoint to $T\sim 10^7$ K, forming an X-ray flare precursor. Then, the pulse of the longitudinal electric current leaves the instability region as a nonlinear Alfvén wave (see Figure 2) with the induced electric field that accelerates electrons to energies sufficient to form a solar flare hard X-ray source. This is a possible scenario for a flare with a precursor [Zaitsev, Stepanov, 2025].

Explore the conditions for the formation of such a prompt flare precursor. First, from (11), find the time of heating of magnetic loop footpoints to $T \geq 10^7$ K by electric currents. We can ignore dissipation due to the Spitzer resistivity since at $\sim 3\cdot 10^{11}$ A such resistivity is significant only for heights <1000 km [Stepanov et al., 2024]. When estimating the heating time, neglect the radiative losses caused by high temperatures, as well as the thermal conductivity along the loop, which is suppressed by a significant azimuthal magnetic field component B_φ associated with the longitudinal current j_z. Assume that at $T>10^6$ K the relative number density of neutrals depends on temperature in the same way as in the quasi-stationary corona, i.e. $F \approx 0.15/T$ [Verner, Ferland, 1996; Zaitsev, 2015]. From the heat balance equation

$$\frac{1}{\gamma - 1}\frac{\partial p}{\partial t} = 2.6\cdot 10^{-9}\frac{I^4}{n^2 a^2 T^{3/2}}, \\ p = 2k_B nT,\ \gamma = \frac{5}{3} \tag{12}$$

determine the temperature dependence on time

$$T^{5/2} - T_0^{5/2} = 3.25\cdot 10^{-9}(\gamma - 1)\frac{I^4}{k_B n^3 a^6} t. \tag{13}$$

From (13), find the heating time of the chromospheric footpoints $t_H \approx 10^4\,\text{s} \sim 3$ hr to $T \geq 10^7$ K at $I = 10^{12}$ A, $n = 4\cdot 10^{11}$ cm^{-3} and $a = 3\cdot 10^7$ cm. Such a long heating time means that we cannot use the formula for the relative number density of neutrals for the quasi-stationary corona, but we should take into account the

pulsed nature of heating and the nonstationarity of ionization process. The rate of change in the plasma electron density during neutral atom ionization by electron impact can be estimated from the equation

$$\frac{dn}{dt} = nn_a \langle \sigma_H V_{Te} \rangle. \quad (14)$$

The hydrogen atom ionization cross-section $\sigma_H \approx 2\cdot10^{-17}$ cm^2 at $T \approx 10^7$ K [Andreev, 2010]. The heating time of precursor plasma by electric current $\tau_H \approx 10$ s. During this time, plasma at the loop footpoint is only partially ionized, retaining a certain number of neutrals. The number density of neutrals at the heating stage is estimated from Equation (14):

$$n_a \approx \frac{\partial n/\partial t}{n\langle \sigma_H V_{Te} \rangle} \approx \frac{1}{\tau_H \langle \sigma_H V_{Te} \rangle} \approx 4\cdot10^6 \text{ cm}^{-3}. \quad (15)$$

With the plasma number density $n \approx 4\cdot10^{11}$ cm^{-3} in the precursor generation region, the relative number density of neutrals $F = n_a / n = 10^{-5}$. It is three orders of magnitude higher than the relative number density of neutrals in the corona with $T = 10^7$ K $\left(F \approx 0.15/T \approx 10^{-8}\right)$. This difference is caused by the fact that when a strong electric current is pulsed on the heating rate is higher than the ionization rate (ionization does not keep up with heating). Therefore, when a current pulse "escapes" from the flare precursor region in the form of a nonlinear Alfvén wave, the residual number density of neutrals in this region remains quite high [Zaitsev, Stepanov, 2025]. To determine the current required to heat the precursor to $T \approx 10^7$ K during the time τ_H 10 s at $F \approx 10^{-5}$, we use Equation (12) from which we find the heating time.

$$\tau \approx \frac{1.6\cdot10^{-8} n^3 a^6 T^{3/2}}{FI^4} \text{ s}. \quad (16)$$

It follows from (16) that for the region with $n = 4\cdot10^{11}$ cm^{-3}, $a = 3\cdot10^7$ cm, $F = 10^{-5}$ plasma heating to $T \approx 10^7$ K during the time $\tau_H \le 10$ s is possible at $I \ge 10^{12}$ A. For the plasma number density $n = 10^{11}$ cm^{-3}, the critical current $I \ge 5\cdot10^{11}$ A. Such electric currents are recorded in flare precursors [Wang et al., 2017]. Since the heating time is $\sim I^{-4}$, prompt X-ray precursors at currents lower than 10^{11} A are unlikely to exist.

CONCLUSION

We have shown that the Rayleigh — Taylor instability is a flare trigger both at loop footpoints and at their tops. RTI at the loop footpoint leads to the intrusion of the surrounding chromospheric plasma into the loop at a velocity $\sim V_{Ti}$ during the time $\sim a/V_{Ti}$ ~10 s, with the longitudinal electric current increasing $I_z = I_0 \exp\left(\frac{2}{a}\int_0^t V(t')dt'\right)$. Joule dissipation with increased Cowling resistivity causes the chromosphere to heat up at loop footpoints and a significant number of electrons to accelerate to energies ~1–3 MeV in induced electric fields. At the same time, for ~10^{38}–10^{39} electrons to accelerate during a flare, electric fields should be either close to the Dreicer field or higher (super-Dreicer). Our results on energy release and particle acceleration in the chromosphere can be considered as *déjà vu* — return to the concept of a chromospheric flare.

The Rayleigh — Taylor instability at tops of flare loops, loaded with a dense cold filament, initiates phenomena similar to those described for loop footpoints. In this case, the filament injects a significant number of neutral particles into current-carrying magnetic loops, which dramatically increase the Joule dissipation at loop tops, accompanied by charged particle acceleration. Thus, we can explain flares of the "above-the-loop-top" type [Masuda et al., 1994] in the current-carrying magnetic loop model.

An important consequence of RTI as a solar flare trigger is the possibility of explaining prompt (~10 s) hot (10–15 MK) solar flare precursors. We have shown that if the pulse current exceeds 10^{11}A, the Joule plasma heating rate overtakes the ionization rate, which leads to increased electric current dissipation. Note that preheating of flare plasma to a temperature >12 MK is also a necessary condition for accelerating high-energy (>100 MeV) protons [Struminsky et al., 2024]. Moreover, understanding the physical nature of the solar flare trigger is of paramount importance for predicting space weather and mitigating its impact on technological infrastructure.

The work was financially supported by RSF (Grant No. 22-12-00308-P).

REFERENCES

Alfvén H., Carlqvist P. Currents in the solar atmosphere and a theory of solar flares. *Solar Phys*. 1967, vol. 1, p. 220–228. DOI: 10.1007/BF00150857.

Andreev G.V. Calculation of ionization cross-section by electron shock for hydrogen and nitrogen atoms. *Physical-Chemical Kinetics in Gas Dynamics*. 2010, vol. 9, pp. 1–2. (In Russian).

Awasthi A.K., Jain R. Multi-wavelength diagnostics of precursor phase in solar flares. *First Asia-Pacific Solar Physics Meeting. Astron. Soc. India Conf*. 2011, vol. 2, pp. 297–305.

Battaglia A.F., Hudson H., Warmuth A., et al. The existence of hot X-ray onsets in solar flares. *Astron. Astrophys*. 2023, vol. 679, article number A139. DOI: 10.1051/0004-6361/202347706.

Brown J.C. On the ionization of hydrogen in optical flares. *Solar Phys*. 1973, vol. 29, pp. 421–427. DOI: 10.1007/BF00150822.

da Silva D. F., Hui L., Simoes P.J.A., et al. Statistical analysis of the onset temperature of solar flares in 2010–2011. *Monthly Notices of the Royal Astronomical Society*. 2023, vol. 525, iss. 3, pp. 4143–4148. DOI: 10.1093/mnras/stad2244.

Emslie A.G., Henoux J.-C. The electrical current structure associated with solar flare electrons accelerated by large-scale electric fields. *Astrophys. J*. 1995, vol. 446, p. 371. DOI: 10.1086/175796.

Fritzová-Švestková L., Švestka Z. Electron density in flares. II Results of measurement. *Solar Phys*. 1967, vol. 2, pp. 87–97. DOI: 10.1007/BF00155894.

Giovanelli R.G. A theory of chromospheric flares. *Nature*. 1946, vol. 158, pp. 81–82. DOI: 10.1038/158081a0.

Hoyng P., Brown J.C., van Beek H.F. High time resolution analysis of solar hard X-ray flares observed on board the ESRO TD-1A satellite, *Solar Phys.* 1976, vol. 48, P.197–254. DOI: 10.1007/BF00151992.

Hudson H., Simoes P.J.A., Fletcher L., et al. Hot X-ray onsets of solar flares. *Monthly Notices of the Royal Astronomical Society*. 2021, vol. 501, iss. 1, pp. 1273–1281. DOI: 10.1093/ mnras/staa3664.

Kane S.R., Hurley K., McTiernan J.M., et al. Energy release and dissipation during giant solar flares. *Astrophys. J. Lett*. 1995, vol. 446, p. L47. DOI: 10.1086/187927.

Kumar P., Srivastava A.K., Somov, B.V., et al. Evidence of solar flare triggering due to loop-loop interaction caused by footpoint shear motion. *Astrophys. J.* 2010, vol. 723, pp. 1651–1664. DOI: 10.1088/0004-637X/723/2/1651.

Kusano K., Bamba Y., Yamamoto T.T. Magnetic field structures triggering solar flares and coronal mass ejections. *Astrophys. J*. 2012, vol. 760, no. 1, p. 31. DOI: 10.1088/0004-637X/760/1/31.

Ledentsov L. Thermal trigger for solar flares I: Fragmentation of the preflare current layer. *Solar Phys.* 2021, vol. 296, article number 74. DOI: 10.1007/s11207-021-01817-1.

Masuda S., Kosugi T., Hara H., et al. A loop-top hard X-ray source in a compact solar flare as evidence for magnetic reconnection. *Nature*. 1994, vol. 371, pp. 495–497. DOI: 10.1038/371495a0.

Meshalkina N.S., Altyntsev A.T. Heating manifestations at the onset of the 29 June 2012 flare. *Solar-Terrestrial Physics*. 2024, vol. 10, iss. 3, pp/ 1–17. DOI: 10.12737/stp-103202402.

Melrose D.B. Neutralized and unneutralized current patterns in the solar corona. *Astrophys. J*. 1991, vol. 381, p. 306. DOI: 10.1086/170652.

Miller J.A., Cargill P.J., Emslie A.G., et al. Critical issues for understanding particle acceleration in impulsive solar flares. *J. Geophys. Res*. 1997, vol. 102, pp. 14631–14659. DOI: 10.1029/97JA00976.

Pustil'nik L.A. Instability of quiescent prominences and the origin of solar flares. *Soviet Astronomy.* 1974, vol. 17, p. 763.

Sharykin I.N., Kosovichev A.G. Dynamics of electric currents, magnetic field topology, and helioseismic response of a solar flare. *Astrophys. J.* 2015, vol. 808, no.1. DOI: 10.1088/0004-637X/808/1/72.

Somov B.V. Magnetic reconnection and topological trigger in physics of large solar flares. ?2008, vol. 17, no. 2-3, pp. 421–454. DOI: 10.48550/arXiv.0901.4697.

Stepanov A.V., Zaitsev V.V. *Magnetospheres of Active Regions of the Sun and Stars*. Moscow, Fizmatlit Publ., 2018, 387 p. (In Russian).

Stepanov A.V., Zaitsev V.V., Kupriyanova E.G. Features of electric current dissipation in the solar atmosphere. *Geomagnetism and Aeronomy*. 2024, vol. 64, pp. 1203–1214. DOI: 10.1134/S001679322470030.

Struminsky A.B. Sadovsky A.M., Grogoryeva I.Yu. Criteria for forecasting proton events from real time solar observations. *Geomagnetism and Aeronomy*. 2024, vol. 64, no. 2, pp. 139–149. DOI: 10.1134/S0016793223600984.

Syrovatskii S.I. Current sheet characteristics and thermal trigger of solar flares. *Soviet Astronomy Letters*. 1976, vol. 2, p. 13.

Verner D.A., Ferland C.J. Atomic data for astrophysics. I. Radiative recombination rates for H-like, He-like, Li-like, and Na-like ions over a broad range of temperature. *Astrophys. J. Suppl. Ser*. 1996, vol. 103, no. 2, pp. 467–473. DOI: 10.1086/192284.

Veronig A., Vršnak B., Dennis B.R., et al. Investigation of the Neupert effect in solar flares. I. Statistical properties and the evaporation model. *Astron. Astrophys.* 2002, vol. 392, no. 2, pp. 699–712. DOI: 10.1051/0004-6361:20020947.

Wang H., Liu Ch., Ahn K., et al. High-resolution observations of flare precursors in the low solar atmosphere. *Nature Astronomy*. 2017, vol. 1, article number 0085. DOI: 10.1038/s41550-017-0085.

Zaitsev V.V. Ultrafine magnetic structures in the chromosphere. *Geomagnetism and Aeronomy*. 2015, vol. 55, pp. 846–849. DOI: 10.1134/S0016793215070294.

Zaitsev V.V., Stepanov A.V. Towards the circuit theory of solar flares. S*olar Phys.* 1992, vol. 139, pp. 343–356. DOI: 10.1007/BF00159158.

Zaitsev V.V., Urpo S., Stepanov A.V. Temporal dynamics of Joule heating and DC-electric field acceleration in single flare loop. *Astron. Astrophys*. 2000, vol. 357, pp. 1105–1114.

Zaitsev V.V., Stepanov A.V. Particle acceleration and plasma heating in the chromosphere. S*olar Phys.* 2015, vol. 290, pp. 3559–3572. DOI: 10.1007/s11207-015-0731-y.

Zaitsev V.V., Stepanov A.V. On the nature of fast X-ray precursors of solar flares. *Astronomy Lett.* 2025, vol. 51, no. 1. (In print).

Zaitsev V.V., Kronshtadtov P.V., Stepanov A.V. Rayleigh — Taylor instability and excitation of super-Dreicer electric fields in the solar chromosphere. S*olar Phys.* 2016, vol. 291, pp. 3451–3459. DOI: 10.1007/s11207-016-0983-1.

Zaitsev V.V., Stepanov A.V., Kronshtadtov P.V. On the possibility of heating the solar corona by heat fluxes from coronal magnetic structures. *Solar Phys.* 2020, vol. 295, article number 166. DOI: 10.1007/s11207-020-01732-x.

Zimovets I.V., Sharykin I.N., Gan W.Q. Relationships between photospheric vertical electric currents and hard X-ray sources in solar flares: Statistical study. *Astrophys. J.* 2020, vol. 891, no. 2. DOI: 10.3847/1538-4357/ab75be.

The 15th Russian-Chinese Space Weather Workshop. September 9–13, 2024, Institute of Solar-Terrestrial Physics SB RAS, Irkutsk, Russia.

Original Russian version: Stepanov A.V., Zaitsev V.V., published in Solnechno-zemnaya fizika. 2025, vol. 11, no. 3, pp. 125–131. DOI: 10.12737/szf-113202513.

How to cite this article

Stepanov A.V., Zaitsev V.V. The Rayleigh—Taylor instability as a trigger of solar flares. *Solar-Terrestrial Physics*. 2025, vol. 11, iss. 3, pp. 114–119. DOI: 10.12737/stp-113202513.